SOLVING THE FUZZY JOB SHOP SCHEDULING PROBLEM VIA LEARNING APPROACHES

Anonymous authors
Paper under double-blind review

ABSTRACT

The fuzzy job shop scheduling problem (FJSSP) emerges as an innovative extension to the conventional job shop scheduling problem (JSSP), incorporating a layer of uncertainty that aligns the model more closely with the complexities of real-world manufacturing environments. This enhancement, while enhancing its applicability, concurrently escalates the computational complexity of deriving solutions. In the domain of traditional scheduling, neural combinatorial optimization (NCO) has recently demonstrated remarkable efficacy. However, its application to the realm of fuzzy scheduling has been relatively unexplored. This paper aims to bridge this gap by investigating the feasibility of employing neural networks to assimilate and process fuzzy information for the resolution of FJSSP, thereby leveraging the advancements in NCO to enhance fuzzy scheduling methodologies. To this end, we present a self-supervised algorithm for the FJSSP (SS-FJSSP). This algorithm employs an iterative mechanism to refine pseudo-labels, progressively transitioning from suboptimal to optimal solutions. This innovative approach adeptly circumvents the significant challenge of procuring true labels, a common challenge in NCO frameworks. Experiments demonstrate that our SS-FJSSP algorithm yields results on a par with the state-of-the-art methods while achieving a remarkable reduction in computational time, specifically being two orders of magnitude faster.

1 INTRODUCTION

The job shop scheduling problem (JSSP) is a well-established combinatorial optimization problem (COP) that holds both theoretical significance and practical relevance (Zhang et al., 2024). The traditional JSSP describes the processing time in the form of crisp number. However, in real-world manufacturing scenarios, numerous uncertain factors, such as human variability (He et al., 2021) and machine flexibility (Huang et al., 2024), often preclude the accurate specification of processing times. To overcome this limitation, the fuzzy JSSP (FJSSP) has emerged and is attracting increasing attention in the field (Abdullah & Abdolrazzagh-Nezhad, 2014; Lin, 2002). Specifically, in the FJSSP, processing times are represented as fuzzy numbers. These uncertainties diminish the practical applicability of the JSSP.

The existing algorithms for FJSSP are mainly heuristic algorithms (Gendreau & Potvin, 2005). Li et al. (2023) developed a bi-population balancing multiobjective evolutionary algorithm for distributed flexible FJSSP. Gao et al. (2020) devised a differential evolution algorithm with an innovative selection mechanism to to more effectively tackle FJSSP. Li et al. (2020) engineered an enhanced artificial immune system algorithm to address flexible FJSSP. Sun et al. (2019) crafted an effective hybrid cooperative coevolution algorithm aimed at minimizing the fuzzy makespan of flexible FJSSP. The integration of particle swarm optimization and genetic algorithms significantly bolstered the convergence capabilities of the proposed algorithm. Wang et al. (2022) utilized fuzzy relative entropy to transform a multiobjective optimization FJSSP into a single-objective optimization problem and designed a hybrid adaptive differential evolution algorithm to resolve it. Pan et al. (2021) concentrated on the energy-efficient flexible FJSSP and developed a bi-population evolutionary algorithm with feedback mechanisms to address it effectively.

The surge in deep learning has catalyzed the emergence of neural combinatorial optimization (NCO), sparking a burgeoning interest in leveraging learning-based approaches to solve combinatorial optimization problems (COPs) (Bengio et al., 2021; Chen & Tian, 2019; Falkner et al., 2022). Initial forays into this domain focused on foundational COPs. Vinyals et al. (2015) were trailblazers with the pointer network, a novel neural network architecture specifically designed for the traveling salesman problem (TSP), thereby underscoring the potential of neural networks in addressing COPs. Bello et al. (2016) combined neural networks with reinforcement learning for the TSP, achieving near-optimal results. This method, while computationally demanding, reduced reliance on intricate engineering and heuristic design. Kool et al. (2018) further refined the pointer network by incorporating attention mechanisms, resulting in significant enhancements in the performance of both the TSP and the vehicle routing problem (VRP). Nazari et al. (2018) introduced a comprehensive framework that utilized reinforcement learning for the VRP, surpassing traditional heuristics on medium-scale capacitated VRP instances without a substantial increase in computational time. The application of NCO has since expanded into the realm of scheduling problems. Zhang et al. (2020) developed a deep reinforcement learning model that autonomously learned JSSP priority dispatch rules. They also introduced a graph neural network (GNN) for encoding states, outperforming existing dispatch rules. Kotary et al. (2022) presented a deep learning strategy that yielded efficient and accurate JSSP approximations; they integrated Lagrangian duality to manage problem constraints, showcasing the potential for generating high-quality JSSP solutions with minimal computational overhead. Corsini et al. (2024) explored a self-supervised training strategy for JSSP, training generative models on multiple solution samples and using the optimal solution as a pseudo-label, thus eliminating the need for costly ground-truth solutions and overcoming challenges associated with supervised learning. However, all these studies are predicated on deterministic environments, and to date, no research has addressed the fuzzy scheduling problem using learning approaches. In this paper, we aim to investigate whether neural networks can assimilate fuzzy information and apply it to solve the FJSSP, thereby integrating the advancements of NCO into fuzzy scheduling.

The main contributions of this work are as follows:

- We propose a self-supervised algorithm for FJSSP (SS-FJSSP), which can learn fuzzy information and solve fuzzy scheduling problems in a learning approach.
- We employ an iterative refinement process to incrementally transform initially inaccurate labels into authentic ones, effectively addressing the challenge of acquiring true labels in the realm of NCOs.
- Experimental results indicate that the SS-FJSSP algorithm matches the performance of the state-of-the-art methods and significantly reduces computation time, with speeds up to 100 times faster.

2 Preliminaries

2.1 Fuzzy number

Fuzzy numbers are used to represent the processing time for fuzzy scheduling, which is described in this section.

In manufacturing environments, precise processing times are often elusive due to variables such as the diverse skill levels of workers (Shao et al., 2024). While exact durations may not be predictable, experts can often draw on historical data to provide estimated durations (Itoh & Ishii, 1999). To address this unpredictability, a prevalent strategy involves estimating within confidence intervals. When certain values are more likely, opting for a fuzzy interval or number becomes an appropriate choice (Fortemps, 1997).

Assume S is a fuzzy set defined on $\mathbb{R}$, with a membership function $\mu_S : \mathbb{R} \to [0, 1]$. The α-cut of S is defined as $S_\alpha = \{x \in \mathbb{R} : \mu_S(x) \geq \alpha\}$, $\alpha \in (0, 1]$, and the support is $S_0 = \{x \in \mathbb{R} : \mu_S(x) > 0\}$. A fuzzy interval is delineated by its α-cuts being confined, and a fuzzy number $\tilde{N}$, with a compact support and a pronounced modal value, is depicted by closed intervals $\tilde{N}_\alpha = [\underline{n}_\alpha, \bar{n}_\alpha]$.

The triangular fuzzy number (TFN) (Zhu et al., 2020) is frequently utilized in fuzzy scheduling problems. Let $\tilde{A}$ be a TFN denoted as $\tilde{A} = (a_1, a_2, a_3)$, where a_1 and a_3 outline the range of potential values and a_2 signifies the modal value within this range. The membership function of $\tilde{A}$ is articulated as follows:

$$\mu_{\tilde{A}}(x) = \begin{cases} \frac{x-a_1}{a_2-a_1}, & \text{if } a_1 < x \leq a_2, \\ \frac{a_3-x}{a_3-a_2}, & \text{if } a_2 < x < a_3, \\ 0, & \text{otherwise.} \end{cases} \tag{1}$$

Let $\tilde{A} = (a_1, a_2, a_3)$ and $\tilde{B} = (b_1, b_2, b_3)$ represent two TFNs. The operations on these TFNs are defined as follows:

1. Additional Operation. According to (Nguyen et al., 2018), the sum of $\tilde{A}$ and $\tilde{B}$ is as follows:

$$\widetilde{A} + \widetilde{B} = (a_1 + b_1, a_2 + b_2, a_3 + b_3). \tag{2}$$

2. Max Operation. According to (Lei, 2010a), the max operation of $\tilde{A}$ and $\tilde{B}$ is as follows:

$$\max(\tilde{A}, \tilde{B}) = \begin{cases} \tilde{A}, & \text{if } \tilde{A} \geq \tilde{B}, \\ \tilde{B}, & \text{otherwise.} \end{cases} \tag{3}$$

This operation is grounded in a ranking method, and for this paper, we employ the method proposed by (Heilpern, 1992). This method defuzzifies TFNs to crisp numbers, allowing the comparison of these values to determine the relationship between the TFNs, as shown in the following formula:

$$\text{Defuzz}(\tilde{A}) = \frac{a_1 + 2a_2 + a_3}{4}. \tag{4}$$

In addition to the above well-defined operations, this paper also deals with subtraction, division, and other operations on TFNs. Therefore, the defuzzification method defined in Eq. (4) is also applied to these operations, ensuring that the neural network can effectively learn and process the relevant information.

2.2 FJSSP

The FJSSP (Vela et al., 2020) involves a collection of jobs, machines, and operations. Specifically, there are n jobs denoted by set $\mathcal{J}$, m machines represented by set $\mathcal{M}$, and N operations within set $\mathcal{O}$. Each operation $i \in \mathcal{O}$ is associated with a unique job $J_i \in \mathcal{J}$, processed by a specific machine $M_i \in \mathcal{M}$, and has an uncertain processing time denoted by a TFN $\tilde{t}_i$. The operations are linked by a binary relationship $\rightarrow$ that forms chains for each job. If operation i precedes j ($i \rightarrow j$), they share the same job $J_i = J_j$, and no other operation x can exist such that $i \rightarrow x$ or $x \rightarrow j$. Let $\mathcal{S}$ be the set of scheduling scheme; The objective of FJSSP is to minimize the fuzzy makespan, i.e., to find the fuzzy start time $\tilde{s}_i$ for each operation $i \in \mathcal{O}$ to minimize the following objective over all possible schemes:

$$\max_{i \in \mathcal{O}} \tilde{s}_i + \tilde{t}_i \tag{5}$$

$$\text{s.t.} \quad \tilde{s}_i \geq 0, \quad \forall i \in \mathcal{O}, \tag{6}$$

$$\tilde{s}_j \geq \tilde{s}_i + \tilde{t}_i, \quad \text{if } i \rightarrow j, i, j \in \mathcal{O}, \tag{7}$$

$$\tilde{s}_j \geq \tilde{s}_i + \tilde{t}_i \wedge \tilde{s}_i \geq \tilde{s}_j + \tilde{t}_j, \quad \text{if } M_i = M_j, i, j \in \mathcal{O}. \tag{8}$$

To enable the neural network to assimilate the intricate constraint information inherent in the FJSSP, this paper deviates from the conventional mixed-integer linear programming models typically utilized in heuristic algorithms, as referenced by (Tirkolaee et al., 2020). Instead, we adopt the disjunctive graph approach, as introduced by (Van Laarhoven et al., 1992), to effectively model the FJSSP. This methodological choice facilitates a more nuanced representation of the scheduling constraints, enhancing the capacity of network to learn and optimize solutions within this complex domain.

The disjunctive graph $G = (V, A, E)$ characterizes problems as follows:

- $V = \mathcal{O} \cup \{S, T\}$, where S and T denote the starting and ending virtual nodes, respectively, each with a processing time of zero.
- A encompasses ordered pairs (i, j) for $i, j \in \mathcal{O}$ such that $i \rightarrow j$, along with pairs (S, j) for the first operations of all jobs and (i, T) for the last operations, representing the directed connections between operations within the jobs.

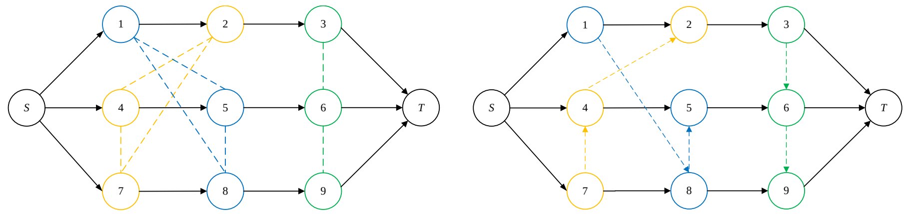

Figure 1: Disjunctive graph model. (a) illustrates a 3 × 3 FJSSP instance. The black solid lines delineate set A, while the colored dashed lines enclose set E. Operations with the same frame color must be executed on the same machine. (b) presents a solution for (a), where all undirected edges have been directed.

- E includes pairs (i, j) where $M_i = M_j$, indicating undirected connections between operations assigned to the same machine.

For each pair of operations $i, j \in \mathcal{O}$ with $i \to j$, the constraint in Eq. (6) is denoted as a directed edge (i, j) in A. Similarly, for each pair of operations $i, j \in \mathcal{O}$ with $M_i = M_j$, the constraint in Eq. (7) is denoted as an undirected edge (i, j) in E, and the two ways of solving the disjunction correspond to the two possible orientations of the edge. Therefore, finding a solution of FJSSP is equivalent to determining the direction of each undirected edge, resulting in a directed acyclic graph. An example of a disjunctive graph for an FJSSP instance and its solution are shown in Figure 1.

Moreover, since the directed edges give constraints on the processing order of all the operations in each job, in decision making, we only need to determine which job (rather than which operation) needs to be processed. For example, Figure 1(b) corresponds to a scheduling scheme $[1, 3, 2, 3, 1, 2, 1, 2, 3]$, and the objective of the algorithm proposed in this paper is to decide on scheduling schemes such as this one and make their fuzzy makespan as small as possible.

3 SS-FJSSP

The SS-FJSSP framework is comprised of two main components, namely an encoder and a decoder. The role of encoder is to assimilate and comprehend the FJSSP information from a holistic standpoint, capturing the broader context and constraints. Subsequently, the decoder leverages the insights gleaned by the encoder to make informed, sequential decisions, breaking down the complex scheduling problem into manageable steps. Moreover, it is essential to preprocess the features of the raw data prior to encoding to enhance the learning process. Each component is described in detail below.

3.1 Feature extraction and encoder

In the disjunctive graph model, the data information, specifically the fuzzy processing times, is stored at the vertices representing the operations, while constraints are defined by the edges. However, the raw data at these vertices, which includes only the individual fuzzy processing times, is insufficient for making accurate decisions. To achieve this, we require more comprehensive information. This is because, in addition to its own numerical magnitude, its role (relative numerical magnitude) in the job and machine to which it belongs is also important. To address this, we employ a feature vector $\boldsymbol{x_i} \in \mathbb{R}^{18}$, associated with operation i, to encapsulate the data information for the entire disjunctive graph. The feature vector $\boldsymbol{x}_i$ contains the following entries:

$$\tilde{t}_i = (t_1, t_2, t_3) \in \mathbb{R}^3, \tag{9}$$

$$\text{Defuzz}\left(\tilde{t}_i\right) \in \mathbb{R}, \tag{10}$$

$$\frac{\sum_{j=\text{St}(i)}^{i} \text{Defuzz}\left(\tilde{t}_j\right)}{\sum_{j=\text{St}(i)}^{\text{End}(i)} \text{Defuzz}\left(\tilde{t}_j\right)} \in \mathbb{R}, \tag{11}$$

$$\frac{\sum_{j=i+1}^{\mathrm{End}(i)} \mathrm{Defuzz}\left(\tilde{t}_j\right)}{\sum_{j=\mathrm{St}(i)}^{\mathrm{End}(i)} \mathrm{Defuzz}\left(\tilde{t}_j\right)} \in \mathbb{R}, \tag{12}$$

$$\mathrm{Quartile}\left(J_i\right) \in \mathbb{R}^3, \tag{13}$$

$$\mathrm{Quartile}\left(M_i\right) \in \mathbb{R}^3, \tag{14}$$

$$\mathrm{Defuzz}\left(\tilde{t}_i\right) - \mathrm{Defuzz}\left(\mathrm{Quartile}\left(J_i\right)\right) \in \mathbb{R}, \tag{15}$$

$$\mathrm{Defuzz}\left(\tilde{t}_i\right) - \mathrm{Defuzz}\left(\mathrm{Quartile}\left(M_i\right)\right) \in \mathbb{R}, \tag{16}$$

where $\mathrm{St}(i)$ and $\mathrm{End}(i)$ denote the the first and last operation of the job that operation i belongs, respectively. $\mathrm{Quartile}(\cdot)$ calculates the quartiles. Eqs. (9) and (10) describe local information and represent the fuzzy processing time and the defuzzified processing time of $\mathcal{O}_i$, respectively. Other equations describe global information. Eqs. (11) and (12) describe how much of the job to which it belongs has been completed and how much is left after processing $\mathcal{O}_i$, respectively. Eqs. (13) and (14) describe the quartiles of fuzzy processing time for the job and machine to which $\mathcal{O}_i$ belongs, respectively. Eqs. (15) and (16) describe the difference of the defuzzified fuzzy processing time of $\mathcal{O}_i$ and Eqs. (13) and (14), respectively.

Subsequently, a two-layer Graph Attention Network (GAT) (Brody et al., 2021) is employed to extract and learn valuable information from the disjunctive graph, which transforms 18-dimensional $\boldsymbol{x_i}$ into a h-dimensional $\boldsymbol{e_i}$. The primary advantage of $\boldsymbol{e_i}$ over $\boldsymbol{x_i}$ is that it complements the relationship between edges. Furthermore, in order not to weaken the information of the vertices, at each layer of the GAT, the output is concatenated with the original feature vector $\boldsymbol{x_i}$. The formulation of encoder is detailed as follows:

$$\boldsymbol{e_i} = \left[\boldsymbol{x_i} \| \mathrm{ReLU}\left(\mathrm{GAT}_2\left(\left[\boldsymbol{x_i} \| \mathrm{ReLU}\left(\mathrm{GAT}_1\left(\boldsymbol{x_i}, G\right)\right)\right], G\right)\right)\right], \tag{17}$$

where "$\|$" is the concatenation operation.

3.2 Decoder

The decoder is composed of two parts: a state network and a decision network. The former is responsible for updating state, and the latter is responsible for making decisions based on the information provided by the decoder and memory network. The two networks are described below.

1. The state network. The SS-FJSSP makes decisions step by step, and each decision impacts the future. Therefore, after each decision, it is necessary to update the state and convey it to the SS-FJSSP to enhance the accuracy of subsequent decisions.

First, we generate an 11-dimensional context vector $\boldsymbol{c_i}$ $(i = 1, 2, \ldots, n)$ for each job to describe its information. Assuming that $o_{t,i}$ denotes the ready operation of job $\mathcal{J}_i$ at step t, and its predecessor is $o_{t,i} - 1$. The context vector $\boldsymbol{c}_i \in \mathbb{R}^{11}$ contains the following entries:

$$\mathrm{Defuzz}\left(\mathrm{CT}(o_{t,i} - 1)\right) - \mathrm{Defuzz}\left(\mathrm{CT}(M_{o_{t,i}})\right) \in \mathbb{R}, \tag{18}$$

$$\frac{\mathrm{Defuzz}\left(\mathrm{CT}(o_{t,i} - 1)\right)}{\mathrm{Defuzz}\left(\max_{i=1,\ldots,n} \mathrm{CT}(\mathcal{J}_i)\right)} \in \mathbb{R}, \tag{19}$$

$$\mathrm{Defuzz}\left(\mathrm{CT}(o_{t,i} - 1)\right) - \frac{\mathrm{Defuzz}\left(\sum_{i=1}^{n} \mathrm{CT}(\mathcal{J}_i)\right)}{n} \in \mathbb{R}, \tag{20}$$

$$\mathrm{Defuzz}\left(\mathrm{CT}(o_{t,i} - 1)\right) - \mathrm{Defuzz}\left(\mathrm{Quartile}(\mathcal{J})\right) \in \mathbb{R}^3, \tag{21}$$

$$\frac{\mathrm{Defuzz}\left(\mathrm{CT}(M_{o_{t,i}})\right)}{\mathrm{Defuzz}\left(\max_{i=1,\ldots,m} \mathrm{CT}(\mathcal{M}_i)\right)} \in \mathbb{R}, \tag{22}$$

$$\mathrm{Defuzz}\left(\mathrm{CT}(M_{o_{t,i}})\right) - \frac{\mathrm{Defuzz}\left(\sum_{i=1}^{m} \mathrm{CT}(\mathcal{M}_i)\right)}{m} \in \mathbb{R}, \tag{23}$$

$$\mathrm{Defuzz}\left(\mathrm{CT}(o_{t,i} - 1)\right) - \mathrm{Defuzz}\left(\mathrm{Quartile}(\mathcal{M})\right) \in \mathbb{R}^3, \tag{24}$$

where $\mathrm{CT}(\cdot)$ calculate the fuzzy completion time. Eq. (18) describes the relationship between two factors that affect the processing of $o_{t,i}$: whether the predecessor operation is complete and whether the required machine is idle. Eq. (19) measures how close the fuzzy completion time of $J_{o_{t,i}}$ is to the current fuzzy makespan. Eq. (20) measures how early or late the fuzzy completion time of $J_{o_{t,i}}$ is compared to the average fuzzy completion time of all jobs in the current state. Eq. (21) describes the relative fuzzy completion time of $J_{o_{t,i}}$ w.r.t. other jobs. Eq. (22) measures how close the fuzzy completion time of $M_{o_{t,i}}$ is to the current fuzzy makespan. Eq. (23) measures how early or late the fuzzy completion time of $M_{o_{t,i}}$ is compared to the average completion time of all machines in the current state. Eq. (24) describes the relative fuzzy completion time of $M_{o_{t,i}}$ w.r.t. other machines.

Second, the context vectors are advancedly integrated through Eq. (25) to derive the state vectors $\boldsymbol{s_i} \in \mathbb{R}^d (i = 1, 2, \ldots, n)$. These vectors serve as a pivotal input to the decision network, enabling it to make informed decisions effectively.

$$\boldsymbol{s_i} = \mathrm{ReLU}\left(\left[\boldsymbol{c_i}\mathbf{W_1} + \underset{j=1,\ldots,n}{\mathrm{MHA}}(\boldsymbol{c_j}\mathbf{W_1})\right]\mathbf{W_2}\right), \tag{25}$$

where $\mathbf{W_1}$ and $\mathbf{W_2}$ are learnable parameter matrices, and MHA denotes the multi-head attention layer (Vaswani, 2017).

2. The decision network. This network combines the $\boldsymbol{e_{o_{t,i}}}$ generated by the encoder that contains global information about the FJSSP, and the $\boldsymbol{s_i}$ generated by the memory network that contains local state information, to generate the probability of choosing a job for the current decision step. More specifically,

$$z_i = \mathrm{FNN}\left(\left[\boldsymbol{e_{o_{t,i}}} \| \boldsymbol{s_i}\right]\right) \in \mathbb{R}, \tag{26}$$

where FNN denotes the feedforward neural network (Glorot & Bengio, 2010). Then, the probabilities p_i for processing the job $\mathcal{J}_i$ in the current step can be obtained by applying the Softmax function to z_i.

Next, a complete scheduling scheme can be generated based on the probability vector $\boldsymbol{p} = [p_1, p_2, \ldots, p_n]^T$, denoting the probability that each job is selected. Specifically, first, at step 1, a job is randomly selected based on $\boldsymbol{p}$ as the decision for this step. Then, the context vectors and state vectors are updated. Finally, based on the new context vectors and state vectors, the probability vector $\boldsymbol{p}$ for next step is generated. Thus, an autoregressive process is formed until all jobs have completed. Moreover, if a job has completed, its probability is set to 0 by a mask operation at subsequent steps.

3.3 Training strategy

Since the FJSSP is an NP-Hard problem (Vela et al., 2020), obtaining true labels is impractical, and this results in the difficulty of solving this problem with a learning approach. Inspired by the work of (Corsini et al., 2024), we overcome this difficulty in the following ways. For each FJSSP instance, we generate α solutions through α parallel decision-making processes and select the appropriate solution as the pseudo-label to minimize the following loss function:

$$\mathcal{L}(\pi, \hat{\pi}) = -\frac{1}{mn}\sum_{t=1}^{mn}\log(p_{t,y_t}), \tag{27}$$

where π and $\hat{\pi}$ denote the scheduling scheme of the pseudo-label and the predicted scheduling scheme of the algorithm, respectively. y_t denotes the t-th job of π, and p_{t,y_t} denotes the probability of the t-th job of π is y_t.

Let P_p represent the perturbation probability. In deviation from the conventional approach of selecting an optimal solution that minimizes the makespan, as proposed by (Corsini et al., 2024), we implement an alternative methodology for determining the suitable solution.

Case 1: If $\mathrm{rand}(0, 1) \geq P_p$. Similar to (Corsini et al., 2024), we select the optimal solution as the pseudo-label.

Case 2: If $\mathrm{rand}(0, 1) < P_p$. Instead of selecting the optimal solution, we randomly select one of the α parallel solutions (which are suboptimal) as the pseudo-label.

The original method anticipates that as the algotirhm learns over time, its predictions will progressively refine, with the pseudo-labels it generates increasingly approximating the true labels, ultimately converging upon them. However, this ideal is unattainable, as depicted in the schematic diagram in Figure 2 (a). For the sake of clarity, we shall assume that the algorithm requires only

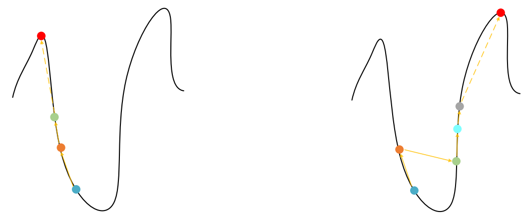

(a) Learning without perturbation (b) Learning with perturbation

Figure 2: Illustration of the learning process. (a) illustrates the learning process without the influence of perturbations. initially at step 0, the algorithm is anchored at the blue point, using the orange point as the initial pseudo-label for learning. By step 1, the focus shifts to the green point, which the algorithm adopts as the new pseudo-label for further learning. This process continues, with the algorithm progressively converging towards a local optimum, represented by the red point. (b) illustrates the learning process with the influence of perturbations. With the introduction of perturbation at step 1, the algorithm is diverted from the peak associated with the local optimum. It opts for a green point, which is not the best option, but it is at the peak where the global optimum is located. As learning progresses, the algorithm moves towards the blue and grey points, ultimately settling at the globally optimal red point.

a single learning iteration to accomplish the acquisition of pseudo-labels. Initially, the algorithm gravitates toward a pseudo-label that approximates a local optimum. While this learning process enhances the predictive capability of algorithm for generating better pseudo-labels, it remains confined to the vicinity of the local optimum, failing to explore the broader landscape for a global optimum. Eventually, the pseudo-label tends to converge towards a local optimum, guiding the learning of algorithm in the same direction. This phenomenon is prevalent due to the solution space being a complex, multi-modal function, where it is nearly impossible to obtain solutions close to the global optimum within a single iteration (LeCun et al., 2015). Thus, we introduce a perturbation, as illustrated in Figure 2 (b). This perturbation enables the algorithm to escape the local optimum during the second learning phase, steering it towards peaks that are closer to the global optimum, and ultimately leading to convergence at the global optimum (true label). It is evident that the perturbation significantly enhances the probability of discovering the true label.

3.4 Further analysis

Every COP can be envisioned as a decision-making process occurring on a graph (Korte et al., 2011), a foundational concept for the SS-FJSSP algorithm. This algorithm iteratively refines its decision-making skills on such graphs. The process is analogous to human decision-making: once the problem is understood, decisions are made incrementally, with each subsequent decision informed by the consequences of its predecessors to enhance accuracy. In this framework, comprehending the problem is the role of the encoder, considering the impact of previous decisions is the function of the state network, and the act of making decisions is the task of the decision network.

Next, the crux of the challenge is teaching the SS-FJSSP algorithm to learn the correct scheduling strategy, enabling it to identify the optimal solution once the problem is understood. This is a feat that humans are currently unable to achieve. The primary obstacle is the NP-Hard nature of the problem, which means an insufficient number of correct labels for the SS-FJSSP to learn from. To overcome this, we draw on the idea of genetic algorithm (Mitchell, 1998): instead of learning the true labels directly, we start with suboptimal labels and gradually approximate the true labels. The core of what makes this strategy work is that even though we do not know if a solution is a true label, for any two solutions, we can distinguish which of them is better (according to the magnitude of the fuzzy makespan).

Specifically, initially, the SS-FJSSP starts without any prior knowledge, randomly generating solutions as potential alternative labels. From these, the most optimal solution is chosen as the pseudo-label, allowing the algorithm to learn. Subsequently, armed with the knowledge acquired previously, the algorithm shows a tendency to predict better alternative labels, leading to the selection of an improved pseudo-label. Repeating this process, ideally, the true label will be selected as the pseudo-label, and the algorithm will eventually learn to make decisions that correspond to it. However, the ideal scenario described above is so perfect that it is nearly unattainable in practice without introducing perturbations. The rationale behind this is that the aforementioned process is essentially akin to a genetic algorithm that employs only crossover without any mutation. Ideally, we anticipate that a superior solution would consistently generate new solutions that are at least as good as the existing ones, thus eventually leading to the global optimum. However, this ideal condition is met if and only if the solution space possesses particularly advantageous properties. In reality, the solution spaces of COPs or neural networks are often complex and multi-modal (LeCun et al., 2015). Consequently, we introduce a perturbation to emulate the role of mutation, which aids the algorithm in escaping local optima and identifying the global optimum, or the true label, as the pseudo-label.

Finally, it becomes evident that with minimal adjustments, this algorithm can be extended to other COPs. This adaptability stems from the fact that any COP can be effectively solved using GNNs once the problem is understood. In terms of decision-making, for any given COP, we are capable of determining the superior label, thereby approximating the true label as outlined in our strategy. Thus, this approach can be regarded as an innovative paradigm for addressing COPs, complementing existing methodologies such as mathematical methods (Ku & Beck, 2016), heuristic methods (Van Laarhoven et al., 1992), and reinforcement learning methods (Zhang et al., 2020).

4 Numerical results and comparison

The SS-FJSSP algorithm is developed using Python 3.9 and PyTorch 1.3.1, and is executed on an Ubuntu 22.04 PC. The hardware setup includes an Intel Platinum 8358P processor and an NVIDIA GeForce RTX 4090 with 24GB of memory.

4.1 Dataset and Test Instances

We randomly generated 30000 instances as the training set by following (Li et al., 2021). The size ($m \times n$) of the training set is 10 × 10, 15 × 10, 15 × 15, 20 × 10, 20 × 15, and 20 × 20, each with 5000 instances. The validation set is generated in the same way as the training set, except that the number of each size is 100. In order to test the performance of SS-FJSSP, we select 2 benchmarks: S (Sakawa & Mori, 1999; Sakawa & Kubota, 2000), and FT (Palacios et al., 2016). We also conducted the experiments for other popular benckmarks such as La (Palacios et al., 2016). The corresponding experimental results are deferred to Appendix.

4.2 Architecture and Training

In the encoder, we utilize two GATs, each equipped with 3 attention heads and a LeakyReLU slope of 0.15. In GAT_1, the size of each head is set to 64 and their outputs are concatenated. In GAT_2, the size of each head is set to 128 and their outputs are averaged. Therefore, $h = 18 + 128 = 146$ and $\boldsymbol{e_i} \in \mathbb{R}^{146}$. In the state network, the size of each head in MHA layer is set to 64 and their outputs are concatenated. This results in parameter matrices $\mathbf{W_1} \in \mathbb{R}^{11\times 192}$ and $\mathbf{W_2} \in \mathbb{R}^{192\times 128}$. Therefore, $d = 128$ and $\boldsymbol{s_i} \in \mathbb{R}^{128}$. In the decision network, the FNN is implemented by a dense layer of 128 neurons, with a final layer of 1 neuron and Leaky-ReLU (slope = 0.15) activation function.

We utilize the Adam optimizer (Kingma, 2014) for training the SS-FJSSP algorithm. The training parameters are set as follows: the number of epochs to 30 and the learning rate to 0.0002. The batch size is configured at 16. Regarding the number of parallel solutions, denoted by α, we set it to 128 during training and increase it to 2048 for testing. Additionally, the perturbation probability, P_p, is established at 0.05.

4.3 Performance on benckmarks

In our evaluation, we have compared our SS-FJSSP with the state-of-the-art method in the field: Constraint Programming (CP), as detailed by (Afsar et al., 2023). As the code for CP is not open-source, our comparison is solely based on the results presented in (Afsar et al., 2023). Their experimental setup included the use of IBM ILOG CP Optimizer version 12.9 on a PC equipped with an Intel Xeon Gold 6132 processor, which operates at 2.6 GHz and is supported by 128 GB of RAM. The operating system utilized was Linux CentOS version 6.9.

Table 1: The comparison results of S-benchmark between SS-FJSSP and CP

Size	Instance	SS-FJSSP		CP	
		FMS	RT	FMS	RT
6×6	S6.1	**(56,80,103)**	**0.06**	**(56,80,103)**	5
	S6.2	**(51,70,86)**	**0.06**	**(51,70,86)**	2
	S6.3	**(51,65,84)**	**0.06**	**(51,65,84)**	3
	S6.4	**(27,36,45)**	**0.07**	**(27,36,45)**	3
10×10	S10.1	(93,135,137)	**0.21**	**(96,129,161)**	36
	S10.2	(92,122,161)	**0.21**	**(92,120,163)**	140
	S10.3	**(85,116,143)**	**0.21**	**(85,116,143)**	43
	S10.4	**(28,47,64)**	**0.36**	**(28,47,64)**	87

Table 2: The comparison results of FT-benchmark between SS-FJSSP and CP

Size	Instance	SS-FJSSP		CP	
		FMS	RT	FMS	RT
6×6	FT06_F	**(54,55,56)**	**0.06**	**(54,55,56)**	55.00
	FT06_G	**(52,55,61)**	**0.06**	**(52,55,61)**	55.75
	FT06_L	**(44,57,73)**	**0.06**	**(44,57,73)**	56.25
	FT06_T	**(42,55,69)**	**0.06**	**(42,55,69)**	55.25
10×10	FT10_F	(917,967,1017)	**0.21**	**(882,930,989)**	932.75
	FT10_G	(892,962,1079)	**0.21**	**(865,930,1058)**	945.75
	FT10_S	(873,960,1074)	**0.20**	**(844,930,1047)**	937.75
20×5	FT20_F	(1157,1232,1307)	**0.33**	**(1094,1165,1238)**	1165.50
	FT20_G	(1129,1223,1141)	**0.33**	**(1074,1165,1356)**	1190.00
	FT20_T	(1176,1231,1288)	**0.33**	**(1112,1165,1216)**	1164.50

Table 1 presents the experimental results on the S-benchmark, with FMS denoting the fuzzy makespan and RT signifying the running time. Notably, in six of the eight instances, our SS-FJSSP algorithm achieves a fuzzy makespan equivalent to that of CP, while significantly reducing the running time. Furthermore, in instances S10.1 and S10.2, the difference in fuzzy makespan between SS-FJSSP and CP is minimal, less than 3%, and the running time of SS-FJSSP is markedly superior, exceeding that of CP by more than 170 times. Table 2 illustrates the experimental results from the FT-benchmark, with notable findings highlighted. Specifically, in the 6×6 instances, the SS-FJSSP algorithm matches the fuzzy makespan of CP while operating at an impressive 900 times faster speed. For all other instances, the fuzzy makespan of SS-FJSSP exceeds that of CP by a maximum of 6%, and it runs at least 3000 times more quickly.

In conclusion, SS-FJSSP is a competitive algorithm despite the differences in experimental settings. Its significant advantage in terms of running time is mainly because it has effectively learned a collection of scheduling rules. For every new operation, SS-FJSSP merely needs to apply the rule once more, ensuring that the running time scales linearly with the complexity of problem. This is an advantage of learning-based approaches. On the other hand, methods such as CP solve problems through an iterative approach. As the problem size escalates, the solution space expands exponentially, a phenomenon known as combinatorial explosion. This exponential growth in the solution space typically results in prolonged running time for these methods.

5 Conclusion

In this paper, we introduce the SS-FJSSP, a self-supervised algorithm tailored to solve the FJSSP. Our in-depth analysis of its workings positions this approach as an innovative paradigm for addressing COPs. Exrensive experiments have demonstrated the effectiveness of the algorithm proposed in this paper. We believe that our proposed algorithm can be extended to other fuzzy scheduling problems, such as the fuzzy flow shop scheduling problem (Deng et al., 2023), and we regard this as a promising avenue for future research.

References

Salwani Abdullah and Majid Abdolrazzagh-Nezhad. Fuzzy job-shop scheduling problems: A review. *Information Sciences*, 278:380–407, 2014.

Sezin Afsar, Camino R Vela, Juan José Palacios, and Inés González-Rodríguez. Mathematical models and benchmarking for the fuzzy job shop scheduling problem. *Computers & Industrial Engineering*, 183:109454, 2023.

Irwan Bello, Hieu Pham, Quoc V Le, Mohammad Norouzi, and Samy Bengio. Neural combinatorial optimization with reinforcement learning. *arXiv preprint arXiv:1611.09940*, 2016.

Yoshua Bengio, Andrea Lodi, and Antoine Prouvost. Machine learning for combinatorial optimization: a methodological tour d'horizon. *European Journal of Operational Research*, 290(2): 405–421, 2021.

Shaked Brody, Uri Alon, and Eran Yahav. How attentive are graph attention networks? *arXiv preprint arXiv:2105.14491*, 2021.

Xinyun Chen and Yuandong Tian. Learning to perform local rewriting for combinatorial optimization. *Advances in neural information processing systems*, 32, 2019.

Andrea Corsini, Angelo Porrello, Simone Calderara, and Mauro Dell'Amico. Self-labeling the job shop scheduling problem. *arXiv preprint arXiv:2401.11849*, 2024.

Libao Deng, Yuanzhu Di, and Ling Wang. A reinforcement-learning-based 3-d estimation of distribution algorithm for fuzzy distributed hybrid flow-shop scheduling considering on-time-delivery. *IEEE Transactions on Cybernetics*, 2023.

Jonas K Falkner, Daniela Thyssens, Ahmad Bdeir, and Lars Schmidt-Thieme. Learning to control local search for combinatorial optimization. In *Joint European Conference on Machine Learning and Knowledge Discovery in Databases*, pp. 361–376. Springer, 2022.

Philippe Fortemps. Jobshop scheduling with imprecise durations: a fuzzy approach. *IEEE Transactions on Fuzzy Systems*, 5(4):557–569, 1997.

Da Gao, Gai-Ge Wang, and Witold Pedrycz. Solving fuzzy job-shop scheduling problem using de algorithm improved by a selection mechanism. *IEEE Transactions on Fuzzy Systems*, 28(12): 3265–3275, 2020.

Michel Gendreau and Jean-Yves Potvin. Metaheuristics in combinatorial optimization. *Annals of Operations Research*, 140:189–213, 2005.

Xavier Glorot and Yoshua Bengio. Understanding the difficulty of training deep feedforward neural networks. In *Proceedings of the thirteenth international conference on artificial intelligence and statistics*, pp. 249–256. JMLR Workshop and Conference Proceedings, 2010.

Lijun He, Raymond Chiong, Wenfeng Li, Sandeep Dhakal, Yulian Cao, and Yu Zhang. Multiobjective optimization of energy-efficient job-shop scheduling with dynamic reference point-based fuzzy relative entropy. *IEEE Transactions on Industrial Informatics*, 18(1):600–610, 2021.

Stanisław Heilpern. The expected value of a fuzzy number. *Fuzzy sets and Systems*, 47(1):81–86, 1992.

Ming Huang, Sihan Huang, Baigang Du, Jun Guo, and Yibing Li. Fuzzy superposition operation and knowledge-driven co-evolutionary algorithm for integrated production scheduling and vehicle routing problem with soft time windows and fuzzy travel times. *IEEE Transactions on Fuzzy Systems*, 2024.

Takeshi Itoh and Hiroaki Ishii. Fuzzy due-date scheduling problem with fuzzy processing time. *International Transactions in Operational Research*, 6(6):639–647, 1999.

Diederik P Kingma. Adam: A method for stochastic optimization. *arXiv preprint arXiv:1412.6980*, 2014.

Wouter Kool, Herke Van Hoof, and Max Welling. Attention, learn to solve routing problems! *arXiv preprint arXiv:1803.08475*, 2018.

Bernhard H Korte, Jens Vygen, B Korte, and J Vygen. *Combinatorial optimization*, volume 1. Springer, 2011.

James Kotary, Ferdinando Fioretto, and Pascal Van Hentenryck. Fast approximations for job shop scheduling: A lagrangian dual deep learning method. In *Proceedings of the AAAI Conference on Artificial Intelligence*, volume 36, pp. 7239–7246, 2022.

Wen-Yang Ku and J Christopher Beck. Mixed integer programming models for job shop scheduling: A computational analysis. *Computers & Operations Research*, 73:165–173, 2016.

Yann LeCun, Yoshua Bengio, and Geoffrey Hinton. Deep learning. *nature*, 521(7553):436–444, 2015.

Deming Lei. Fuzzy job shop scheduling problem with availability constraints. *Computers & Industrial Engineering*, 58(4):610–617, 2010a.

Deming Lei. Solving fuzzy job shop scheduling problems using random key genetic algorithm. *The International Journal of Advanced Manufacturing Technology*, 49:253–262, 2010b.

Jun-qing Li and Yu-xia Pan. A hybrid discrete particle swarm optimization algorithm for solving fuzzy job shop scheduling problem. *The International Journal of Advanced Manufacturing Technology*, 66:583–596, 2013.

Jun-qing Li, Zheng-min Liu, Chengdong Li, and Zhi-xin Zheng. Improved artificial immune system algorithm for type-2 fuzzy flexible job shop scheduling problem. *IEEE Transactions on Fuzzy Systems*, 29(11):3234–3248, 2020.

Junqing Li, Yuyan Han, Kaizhou Gao, Xiumei Xiao, and Peiyong Duan. Bi-population balancing multi-objective algorithm for fuzzy flexible job shop with energy and transportation. *IEEE Transactions on Automation Science and Engineering*, 2023.

Wenfeng Li, Lijun He, and Yulian Cao. Many-objective evolutionary algorithm with reference point-based fuzzy correlation entropy for energy-efficient job shop scheduling with limited workers. *IEEE Transactions on Cybernetics*, 52(10):10721–10734, 2021.

Feng-Tse Lin. Fuzzy job-shop scheduling based on ranking level (/spl lambda/, 1) interval-valued fuzzy numbers. *IEEE Transactions on Fuzzy Systems*, 10(4):510–522, 2002.

Melanie Mitchell. *An introduction to genetic algorithms*. MIT press, 1998.

Mohammadreza Nazari, Afshin Oroojlooy, Lawrence Snyder, and Martin Takác. Reinforcement learning for solving the vehicle routing problem. *Advances in neural information processing systems*, 31, 2018.

Hung T Nguyen, Carol Walker, and Elbert A Walker. *A first course in fuzzy logic*. Chapman and Hall/CRC, 2018.

Juan José Palacios, Jorge Puente, Camino R Vela, and Ines Gonzalez-Rodriguez. Benchmarks for fuzzy job shop problems. *Information Sciences*, 329:736–752, 2016.

Zixiao Pan, Deming Lei, and Ling Wang. A bi-population evolutionary algorithm with feedback for energy-efficient fuzzy flexible job shop scheduling. *IEEE Transactions on Systems, Man, and Cybernetics: Systems*, 52(8):5295–5307, 2021.

Masatoshi Sakawa and Ryo Kubota. Fuzzy programming for multiobjective job shop scheduling with fuzzy processing time and fuzzy duedate through genetic algorithms. *European Journal of operational research*, 120(2):393–407, 2000.

Masatoshi Sakawa and Tetsuya Mori. An efficient genetic algorithm for job-shop scheduling problems with fuzzy processing time and fuzzy duedate. *Computers & industrial engineering*, 36(2): 325–341, 1999.

Zhongshi Shao, Weishi Shao, Jianrui Chen, and Dechang Pi. Mql-mm: A meta-q-learning-based multi-objective metaheuristic for energy-efficient distributed fuzzy hybrid blocking flow-shop scheduling problem. *IEEE Transactions on Evolutionary Computation*, 2024.

Lu Sun, Lin Lin, Mitsuo Gen, and Haojie Li. A hybrid cooperative coevolution algorithm for fuzzy flexible job shop scheduling. *IEEE Transactions on Fuzzy Systems*, 27(5):1008–1022, 2019.

Erfan Babaee Tirkolaee, Alireza Goli, and Gerhard-Wilhelm Weber. Fuzzy mathematical programming and self-adaptive artificial fish swarm algorithm for just-in-time energy-aware flow shop scheduling problem with outsourcing option. *IEEE transactions on fuzzy systems*, 28(11):2772–2783, 2020.

Peter JM Van Laarhoven, Emile HL Aarts, and Jan Karel Lenstra. Job shop scheduling by simulated annealing. *Operations research*, 40(1):113–125, 1992.

A Vaswani. Attention is all you need. *Advances in Neural Information Processing Systems*, 2017.

Camino R Vela, Sezin Afsar, Juan José Palacios, Ines Gonzalez-Rodriguez, and Jorge Puente. Evolutionary tabu search for flexible due-date satisfaction in fuzzy job shop scheduling. *Computers & Operations Research*, 119:104931, 2020.

Oriol Vinyals, Meire Fortunato, and Navdeep Jaitly. Pointer networks. *Advances in neural information processing systems*, 28, 2015.

Gai-Ge Wang, Da Gao, and Witold Pedrycz. Solving multiobjective fuzzy job-shop scheduling problem by a hybrid adaptive differential evolution algorithm. *IEEE Transactions on Industrial Informatics*, 18(12):8519–8528, 2022.

Cong Zhang, Wen Song, Zhiguang Cao, Jie Zhang, Puay Siew Tan, and Xu Chi. Learning to dispatch for job shop scheduling via deep reinforcement learning. *Advances in neural information processing systems*, 33:1621–1632, 2020.

Cong Zhang, Zhiguang Cao, Wen Song, Yaoxin Wu, and Jie Zhang. Deep reinforcement learning guided improvement heuristic for job shop scheduling. In *The Twelfth International Conference on Learning Representations*, 2024.

You-lian Zheng, Yuan-xiang Li, and De-ming Lei. Swarm-based neighbourhood search for fuzzy job shop scheduling. *International Journal of Innovative Computing and Applications*, 3(3):144–151, 2011.

Guang-Yu Zhu, Chen Ding, and Wei-Bo Zhang. Optimal foraging algorithm that incorporates fuzzy relative entropy for solving many-objective permutation flow shop scheduling problems. *IEEE Transactions on Fuzzy Systems*, 28(11):2738–2746, 2020.

APPENDIX FOR THE PERFORMANCE OF SS-FJSSP ON BENCHMARKS

A PERFORMANCE ON LA-BENCHMARK

The La-benchmark, as introduced in (Palacios et al., 2016), is derived from the JSSP by applying various fuzzification techniques, which are denoted by the final letter of the sample identifier. The corresponding experimental outcomes are presented in Table 3, with a noteworthy upper limit of 21600 seconds set for the running time by the CP method.

The data clearly demonstrates that the SS-FJSSP algorithm possesses a significant advantage in running time, consistently surpassing the CP method by a factor of at least two orders of magnitude across all instances. This superiority is especially pronounced in complex scenarios, such as the LA21_F benchmark, where the SS-FJSSP's performance is significantly enhanced, reaching a remarkable four orders of magnitude faster. Moreover, it is worth highlighting that in almost one-third of the cases, SS-FJSSP matched CP in terms of fuzzy completion time. This not only highlights the algorithm's speed but also its effectiveness, showcasing its competitive edge in both aspects.

Table 3: The comparison results of La-benchmark between SS-FJSSP and CP

Size	Instance	SS-FJSSP		CP	
		FMS	RT	FMS	RT
	La01_G	**(625,666,739)**	**0.10**	**(625,666,739)**	9
	La01_L	**(473,666,862)**	**0.10**	**(501,666,862)**	9
10 × 5	La02_S	(614,677,743)	**0.10**	**(601,655,713)**	41
	La03_G	(557,604,706)	**0.10**	**(549,597,708)**	36
	La05_G	**(548,593,665)**	**0.10**	**(548,593,665)**	11
	La06_L	**(667,926,1186)**	**0.34**	**(667,926,1186)**	76
15 × 5	La07_G	**(821,890,1003)**	**0.19**	**(821,890,1003)**	18
	La09_G	**(869,951,1065)**	**0.19**	**(869,951,1065)**	20
	La11_F	**(1164,1222,1280)**	**0.33**	**(1164,1222,1280)**	41
	La12_F	**(975,1039,1103)**	**0.33**	**(975,1039,1103)**	88
	La12_G	**(968,1039,1204)**	**0.33**	**(968,1039,1204)**	104
20 × 5	La13_F	**(1072,1150,1326)**	**0.33**	**(1072,1150,1228)**	86
	La13_G	**(1070,1150,1326)**	**0.33**	**(1070,1150,1326)**	102
	La14_F	**(1203,1292,1381)**	**0.33**	**(1203,1292,1381)**	106
	La14_G	**(1197,1292,1522)**	**0.33**	**(1197,1292,1522)**	118
10 × 10	La19_S	(765,856,941)	**0.21**	**(752,842,948)**	1097
	La20_Z	(821,916,1053)	**0.21**	**(816,902,1036)**	394
	La21_F	(1046,1122,1198)	**0.39**	**(977,1046,1128)**	5187
	La21_S	(997,1031,1264)	**0.39**	**(943,1046,1167)**	4123
	La21_Z	(1010,1123,1285)	**0.39**	**(943,1046,1196)**	2427
15 × 10	La22_Z	(856,965,1100)	**0.39**	**(833,927,1065)**	282
	La24_F	(911,983,1055)	**0.39**	**(871,937,1010)**	2608
	La24_S	(878,983,1089)	**0.39**	**(840,938,1053)**	1533
	La25_F	(954,1016,1078)	**0.39**	**(913,978,1045)**	4223
	La25_S	(926,1029,1154)	**0.39**	**(882,977,1111)**	18561
	La27_F	(1226,1321,1416)	**0.67**	**(1154,1235,1316)**	6196
20 × 10	La27_S	(1195,1330,1437)	**0.67**	**(1132,1248,1366)**	21600
	La29_F	(1146,1237,1328)	**0.67**	**(1081,1154,1238)**	21600
	La29_S	(1162,1311,1457)	**0.67**	**(1052,1171,1319)**	21600
	La36_S	(1176,1305,1443)	**0.59**	**(1160,1275,1416)**	2931
	La37_S	(1351,1499,1625)	**0.59**	**(1262,1399,1560)**	979
	La38_F	(1187,1272,1357)	**0.59**	**(1128,1196,1284)**	21600
15 × 15	La38_S	(1171,1276,1433)	**0.59**	**(1091,1205,1342)**	21600
	La39_S	(1162,1311,1457)	**0.59**	**(1112,1233,1387)**	825
	La40_F	(1199,1285,1371)	**0.59**	**(1146,1224,1313)**	1013
	La40_S	(1177,1290,1406)	**0.59**	**(1119,1228,1357)**	3458

Table 4: The comparison results of the benchmarks of Lei and LP between SS-FJSSP and CP

Size	Instance	SS-FJSSP		CP	
		FMS	RT	FMS	RT
15 × 10	Lei01	(145,211,280)	**0.39**	**(136,200,259)**	9977
	Lei02	(129,178,226)	**0.55**	**(118,164,214)**	234
16 × 16	LP01	(150,196,250)	**0.69**	**(145,190,246)**	21600

Table 5: The comparison results of the benchmarks of ABZ and ORB between SS-FJSSP and CP

Size	Instance	SS-FJSSP		CP	
		FMS	RT	FMS	RT
10 × 10	ABZ5_Z	(1139,1253,1434)	**0.21**	**(1111,1239,1414)**	876
	ABZ6_G	(882,952,1118)	**0.20**	**(876,943,1068)**	287
	ABZ6_Z	(858,954,1097)	**0.21**	**(842,945,1085)**	363
	ORB01_Z	(1036,1146,1327)	**0.34**	**(961,1060,1215)**	1415
	ORB02_Z	(803,901,1023)	**0.45**	**(784,889,1022)**	507
	ORB03_Z	(962,1082,1251)	**0.30**	**(900,1005,1151)**	1218
	ORB04_Z	(961,1080,1233)	**0.30**	**(894,1006,1154)**	238
	ORB05_Z	(823,914,1049)	**0.31**	**(800,887,1018)**	260
20 × 15	ABZ7_F	(660,710,760)	**1.00**	**(628,660,703)**	21600
	ABZ8_F	(682,723,764)	**1.00**	**(645,681,726)**	21600
	ABZ9_F	(719,758,797)	**1.15**	**(668,704,758)**	21600

B Performance on the benchmarks of Lei and LP

The Lei-benchmark (Lei, 2010b) and the LP-benchmark (Li & Pan, 2013) are specifically developed for fuzzy scheduling purposes, rather than being derived from fuzzifying crisp problems. These benchmarks, despite their compact size, offer a high degree of complexity, often requiring considerable computational resources for the CP method to find solutions. Although the SS-FJSSP algorithm does not always match the solution quality of CP, it provides nearly identical solutions with remarkable efficiency. The experimental findings are detailed in Table 4.

The slightly inferior solution quality produced by SS-FJSSP may be due to the fact that the training set, which is randomly generated, does not fully capture the intricacies of these carefully designed instances. It is expected that with an improved training set that more accurately reflects the complexity of these benchmarks, SS-FJSSP will be able to produce more satisfactory results.

C Performance on the benchmarks of ABZ and ORB

Both the ABZ-benchmark (Palacios et al., 2016) and the ORB-benchmark (Zheng et al., 2011) originate from the fuzzification of highly intricate original problems, retaining their inherent complexity in the fuzzified versions. As depicted in Table 5, while no instance of SS-FJSSP have been able to match the results of CP, the discrepancy is minimal, and the SS-FJSSP still holds a significant advantage in terms of running time. The suboptimal performance in solution quality is also likely attributable to the training set's insufficient complexity, which fails to encapsulate the full intricacy of these benchmarks.

D Performance on the Ta-benchmark

The Ta-benchmark (Afsar et al., 2023), derived from a fuzzy approach, comprises an extensive collection of instances, totaling 80. The corresponding experimental results are meticulously detailed across two tables: Table 6 and Table 7. These results corroborate the characteristics previously discussed, offering further insight into the performance of the evaluated methods.

Table 6: The comparison results of Ta-benchmark between SS-FJSSP and CP in Part I

Size	Instance	SS-FJSSP		CP	
		FMS	RT	FMS	RT
15 × 15	Ta01_F	(1204,1336,1468)	**0.89**	**(1149,1231,1344)**	450
	Ta02_F	(1220,1313,1406)	**0.90**	**(1152,1245,1342)**	1562
	Ta03_F	(1196,1295,1394)	**0.89**	**(1147,1219,1307)**	2099
	Ta04_F	(1145,1226,1307)	**0.89**	**(1083,1175,1275)**	1831
	Ta05_F	(1201,1290,1379)	**0.89**	**(1158,1224,1319)**	21600
	Ta06_F	(1195,1281,1367)	**0.89**	**(1174,1246,1335)**	21600
	Ta07_F	(1181,1284,1387)	**0.89**	**(1147,1228,1322)**	15011
	Ta08_F	(1201,1285,1396)	**0.89**	**(1134,1218,1327)**	18619
	Ta09_F	(1245,1370,1495)	**0.89**	**(1181,1274,1393)**	11445
	Ta10_F	(1206,1317,1428)	**0.89**	**(1163,1243,1326)**	1882
20 × 15	Ta11_F	(1337,1460,1583)	**1.62**	**(1290,1387,1488)**	21600
	Ta12_F	(1349,1464,1579)	**1.62**	**(1279,1377,1488)**	21600
	Ta13_F	(1360,1452,1544)	**1.62**	**(1312,1413,1536)**	21600
	Ta14_F	(1323,1409,1495)	**1.62**	**(1248,1345,1442)**	1544
	Ta15_F	(1328,1452,1576)	**1.62**	**(1279,1373,1470)**	21600
	Ta16_F	(1355,1480,1605)	**1.62**	**(1283,1381,1492)**	21600
	Ta17_F	(1474,1582,1690)	**1.61**	**(1352,1464,1593)**	1468
	Ta18_F	(1411,1538,1665)	**1.62**	**(1367,1474,1593)**	21600
	Ta19_F	(1351,1446,1541)	**1.62**	**(1250,1378,1507)**	21600
	Ta20_F	(1346,1456,1566)	**1.62**	**(1278,1368,1471)**	21600
20 × 20	Ta21_F	(1672,1792,1912)	**2.16**	**(1596,1697,1824)**	21600
	Ta22_F	(1589,1731,1873)	**2.16**	**(1546,1666,1809)**	21600
	Ta23_F	(1589,1708,1827)	**2.17**	**(1526,1614,1726)**	21600
	Ta24_F	(1663,1788,1913)	**2.16**	**(1579,1708,1847)**	21600
	Ta25_F	(1602,1718,1834)	**2.16**	**(1524,1632,1765)**	21600
	Ta26_F	(1640,1769,1898)	**2.30**	**(1643,1742,1865)**	21600
	Ta27_F	(1736,1844,1952)	**2.16**	**(1664,1780,1914)**	21600
	Ta28_F	(1611,1733,1855)	**2.17**	**(1561,1662,1770)**	21600
	Ta29_F	(1593,1726,1859)	**2.16**	**(1554,1660,1780)**	21600
	Ta30_F	(1593,1726,1859)	**2.17**	**(1545,1647,1756)**	21600
30 × 15	Ta31_F	(1794,1944,2094)	**3.26**	**(1682,1805,1938)**	21600
	Ta32_F	(1872,1994,2116)	**3.27**	**(1690,1824,1979)**	21600
	Ta33_F	(1859,2006,2153)	**3.27**	**(1706,1853,2008)**	21600
	Ta34_F	(1858,1995,2132)	**3.26**	**(1709,1866,2023)**	21600
	Ta35_F	(1895,2067,2239)	**3.27**	**(1847,2007,2167)**	2367
	Ta36_F	(1859,2000,2141)	**3.26**	**(1720,1847,1987)**	21600
	Ta37_F	(1837,1972,2107)	**3.26**	**(1647,1796,1967)**	21600
	Ta38_F	(1692,1839,1986)	**3.27**	**(1575,1692,1847)**	21600
	Ta39_F	(1810,1963,2116)	**3.27**	**(1711,1822,1933)**	21600
	Ta40_F	(1743,1876,2009)	**3.27**	**(1600,1714,1858)**	21600

Table 7: The comparison results of Ta-benchmark between SS-FJSSP and CP in Part II

Size	Instance	SS-FJSSP		CP	
		FMS	RT	FMS	RT
30 × 20	Ta41_F	(2169,2311,2453)	**0.89**	**(1958,2090,2222)**	21600
	Ta42_F	(2011,2167,2323)	**0.90**	**(1862,2032,2205)**	21600
	Ta43_F	(1936,2085,2234)	**0.89**	**(1809,1949,2090)**	21600
	Ta44_F	(2103,2219,2335)	**0.89**	**(1933,2044,2173)**	21600
	Ta45_F	(2058,2191,2324)	**0.89**	**(1928,2036,2170)**	21600
	Ta46_F	(2087,2230,2373)	**0.89**	**(1949,2066,2215)**	21600
	Ta47_F	(1959,2087,2215)	**0.89**	**(1828,1973,2120)**	21600
	Ta48_F	(2036,2199,2362)	**0.89**	**(1881,2012,2160)**	21600
	Ta49_F	(2040,2175,2310)	**0.89**	**(1897,2030,2177)**	21600
	Ta50_F	(2061,2221,2381)	**0.89**	**(1902,2032,2172)**	21600
50 × 15	Ta51_F	(2804,3052,3300)	**1.62**	**(2549,2760,2971)**	21600
	Ta52_F	(2696,2942,3188)	**1.62**	**(2581,2756,2931)**	21600
	Ta53_F	(2628,2852,3076)	**1.62**	**(2521,2717,2915)**	21600
	Ta54_F	(2628,2863,3098)	**1.62**	**(2605,2839,3073)**	21600
	Ta55_F	(2726,2935,3144)	**1.62**	**(2497,2679,2880)**	21600
	Ta56_F	(2707,2921,3135)	**1.62**	**(2574,2781,2994)**	21600
	Ta57_F	(2852,3097,3342)	**1.61**	**(2719,2943,3167)**	21600
	Ta58_F	(2777,3025,3273)	**1.62**	**(2682,2885,3128)**	21600
	Ta59_F	(2683,2900,3117)	**1.62**	**(2469,2655,2865)**	21600
	Ta60_F	(2614,2828,3042)	**1.62**	**(2525,2723,2927)**	21600
50 × 20	Ta61_F	(2857,3099,3341)	**2.16**	**(2691,2868,3072)**	21600
	Ta62_F	(2921,3144,3367)	**2.16**	**(2729,2904,3085)**	21600
	Ta63_F	(2745,2973,3201)	**2.17**	**(2529,2755,2987)**	21600
	Ta64_F	(2601,2823,3045)	**2.16**	**(2495,2702,2909)**	21600
	Ta65_F	(2795,3013,3231)	**2.16**	**(2559,2725,2948)**	21600
	Ta66_F	(2813,3040,3267)	**2.30**	**(2625,2845,3094)**	21600
	Ta67_F	(2753,2994,3235)	**2.16**	**(2606,2826,3083)**	21600
	Ta68_F	(2657,2886,3115)	**2.17**	**(2609,2784,2971)**	21600
	Ta69_F	(2992,3233,3474)	**2.16**	**(2850,3071,3292)**	21600
	Ta70_F	(2991,3273,3555)	**2.17**	**(2792,2995,3219)**	21600
100 × 20	Ta71_F	(5263,5613,5963)	**3.26**	**(5089,5464,5839)**	21600
	Ta72_F	(4901,5264,5627)	**3.27**	**(4822,5181,5540)**	21600
	Ta73_F	(5392,5777,6162)	**3.27**	**(5195,5568,5941)**	21600
	Ta74_F	(4972,5351,5730)	**3.26**	**(4950,5339,5739)**	21600
	Ta75_F	(5342,5710,6078)	**3.27**	**(4959,5392,5830)**	21600
	Ta76_F	(5175,5560,5945)	**3.26**	**(5022,5342,5736)**	21600
	Ta77_F	(5128,5462,5796)	**3.26**	**(5050,5436,5822)**	21600
	Ta78_F	(5137,5498,5859)	**3.27**	**(4980,5394,5808)**	21600
	Ta79_F	(5006,5392,5778)	**3.27**	**(4974,5358,5744)**	21600
	Ta80_F	(4922,5341,5760)	**3.27**	**(4833,5183,5533)**	21600